Proceedings of the 5th WSEAS International Conference on Applied Computer Science, Hangzhou, China, April 16-18, 2006 (pp862-867)

Texture analysis for textile fault detection

A. SPARAVIGNA[1] and B. MONTRUCCHIO[2]
[1] Dipartimento di Fisica, [2] Dipartimento di Automatica ed Informatica
Politecnico di Torino
corso Duca degli Abruzzi 24, I-10129 Torino
ITALY

*preferred author for correspondence

Abstract: - A texture analysis for fault detection on textile surfaces is presented. Peculiarities of the texture formed by the woven fabric are evaluated with an algorithm based on statistical parameters and independent on the image contrast, recently introduced to investigate textures in liquid crystals microscopy. Changes from the regular texture can be monitored comparing parameters of the standard texture with the actual texture recorded by CCD camera.

Key-Words: - image processing, texture analysis, defect detection

1 Introduction

Inspection of woven fabrics is fundamental for textile industry to guarantee its product quality. Nowadays, most of fabric inspections is performed by trained staff on off-line stations. A quality evaluation during the production process, directly on the loom, would be very important for lowering costs and improving quality. Automatic systems based on the artificial vision must perform a very difficult task since faults on fabrics are often very small and hardly detectable, with their visibility strongly dependent on illumination systems (front or back lighting) and reduced by vibrations of the mounting devices [1-3]. Automatic inspections with opto-electronic processing based on diffractive optics have been proposed, but without appreciable influence on direct on-loom inspections [4-5].

Concerning the texture analysis on textile surfaces, several statistical approaches to the image texture analysis have been developed [6-8]. Methods based for instance on the Fourier space representations have also been proposed to measure the spatial frequency of the grey levels [9]. The Fourier methods suffer from the local intensity variation in the image, that can be easily confused with the presence of true defects. Use of wavelets with adaptive bases was also proposed, getting advantages from the wavelet property to analyse the local behavior of the texture in comparison with chosen grey level distributions [10].

In the research field of liquid crystal physics, in studying liquid crystal textures with polarized light microscopy, a method was proposed to characterize the domains appearing in the images [11]. The method was able to detect anomalies in stochastic textures by means of a set of coherence lengths, measuring the domain size. The approach, based on the use of statistical parameters, turns out to be independent on image intensity and contrast.

Since intensity and contrast are crucial points for the image processing on textile surfaces, where dust and vibrations reduce the image quality, we present here a new algorithm based on coherence lengths, characterizing textile textures and monitoring the fault presence in woven structures.

2 The Algorithm

Images are detected by a CCD camera, stored and elaborated on a workstation. We consider grey-level images $g(x,y)$ with pixels $l_x \times l_y$. The mean intensity M_o and the $k-$ rank statistical moments:

$$M_o = \frac{1}{l_x l_y} \sum_{x=0}^{l_x} \sum_{y=0}^{l_y} g(x,y) \qquad (1)$$

$$M_k = \frac{1}{l_x l_y} \sum_{x=0}^{l_x} \sum_{y=0}^{l_y} \left[g(x,y) - M_o \right]^k \qquad (2)$$

of the (x,y) rectangular image frame are evaluated. Starting from an arbitrary point, in a chosen direction, for instance the x- direction, we calculate the mean value of pixel grey tones over a distance l_o:

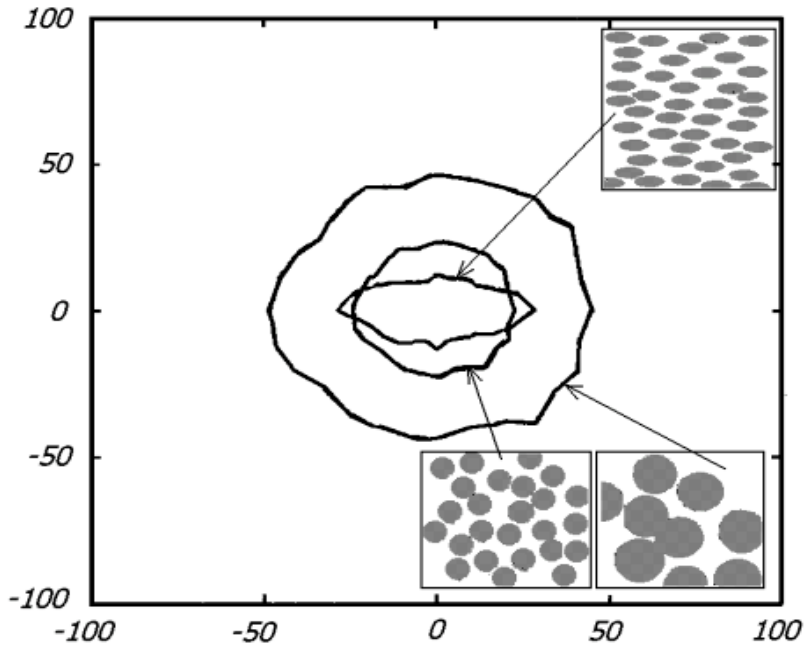

Figure 1: Polar diagram for the coherence lengths of three images. Anisotropy of th e texture is clearly exhibited by polar diagram for ellipses. Units on axes ar e pixels. Images for testing the coherence lengths cover an area of 200 pixels x 200 pixels.

$$M_o^x(x,y)=\frac{1}{l_o}\sum_{\xi=0}^{l_o} g(x+\xi,y) \qquad (3)$$

Distance $l_o = l_o^x(x,y)$ is function of the starting point $P(x,y)$ and defined as the distance where the value of directional moment $M_o^x(x,y)$ reaches, within a threshold level τ, the value of image moment M_o: function $l_o^x(x,y)$ then represents the behavior of local coherence lengths relevant to the mean intensity.

We choose to define these functions as coherence lengths according to their actual use in physics. For instance, coherence length in optics is the propagation distance from a coherent source to a point where an electromagnetic wave maintains a specified degree of coherence. In the liquid crystal physics, coherence length measures the distance where order parameter mantains itself almost constant.

Averaging on the whole image frame,

$$L_o^x = \frac{1}{l_x l_y}\sum_{x=0}^{l_x}\sum_{y=0}^{l_y} l_o^x(x,y) \qquad (4)$$

the mean coherence length L_o^x is obtained. The same procedure is applied in y-direction for coherence L_o^y. Coherence lengths can be evaluated, very conveniently, in any direction, since the weaving process imposes peculiar directions in the fabric structure.

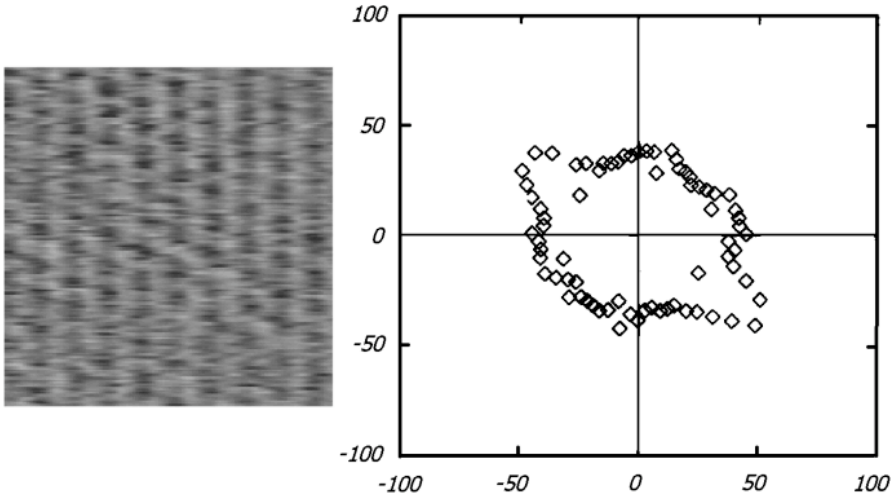

Figure 2: Surface texture of a mica slab observed by means of an atomic force microscope and its polar diagram of coherence lengths. Diagram clearly exhibits the exagonal structure of mica surface.

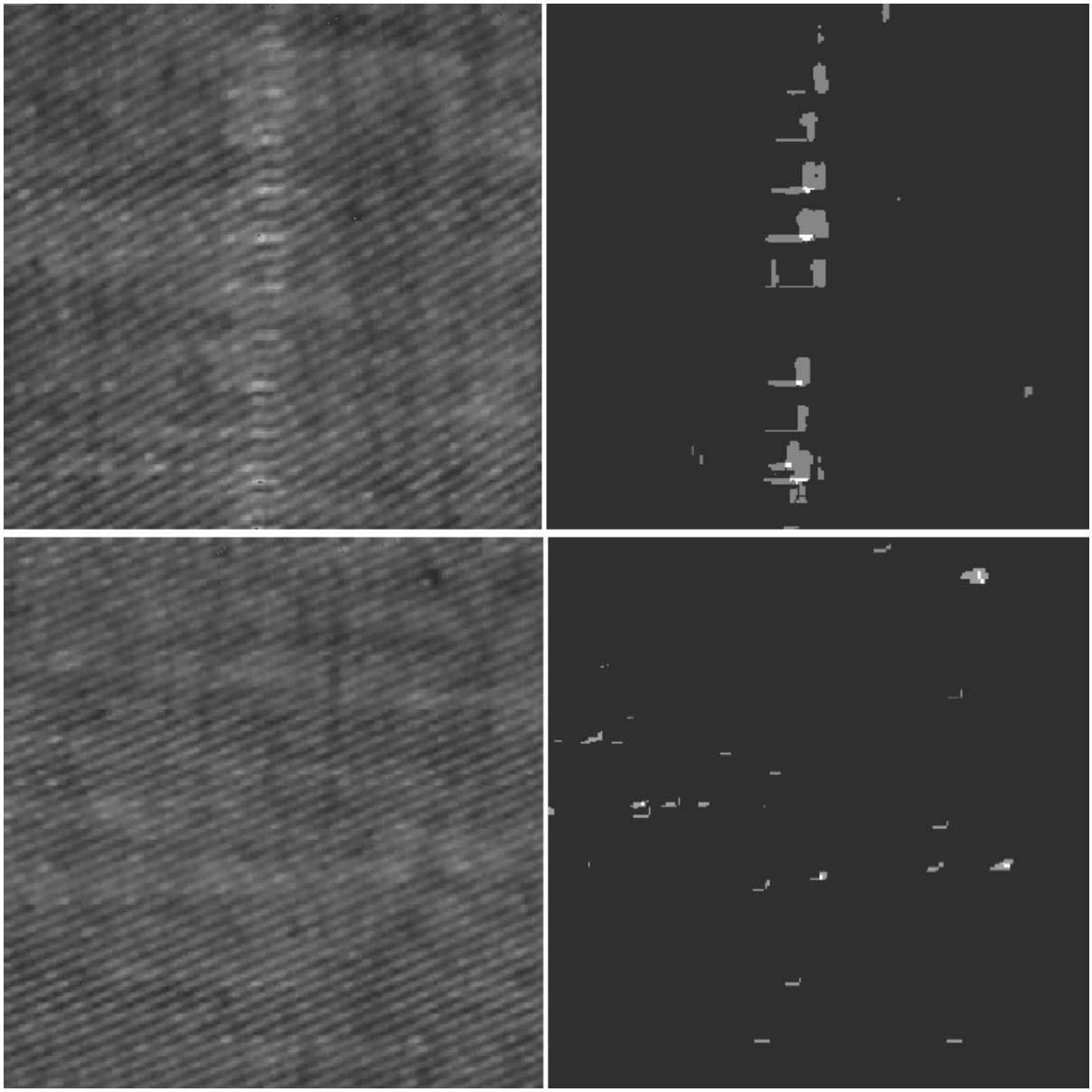

Figure 3: A mispick in a textile woven fabric (upper part) and the corresponding map obtained with the algorithm described in the text. The same fabric (lower part) with dust and oil spots and the corresponding map. Image size is 40 mm.

To illustrate how coherence lengths are able to identify textures placed in an image frame, a few simple examples are considered, with images reproducing circles and ellipses. Coherence lengths in all the directions of the image plane (not only $x-$ and $y-$directions), provide a polar diagram as shown in Fig.1. From the polar diagram, texture dimensions and texture anisotropy receive quantitative evaluations.

Experiments on texture images and polar diagrams (see for instance, Fig.2) allow to conclude that coherence lengths defined by Eq.(4) are able to give domain sizes in the image frame. These coeherence values can then be used for textile surfaces as parameters characterizing the image texture. Let us note that the coherence length evaluation is not depending on the value of mean intensity M_o and on image contrast. Threshold τ is usually chosen as the ratio σ/M_o where σ is the standard deviation of the image grey tones, obtained by the second order moment.

3 Fault detection

Faults in the structure of woven fabrics are

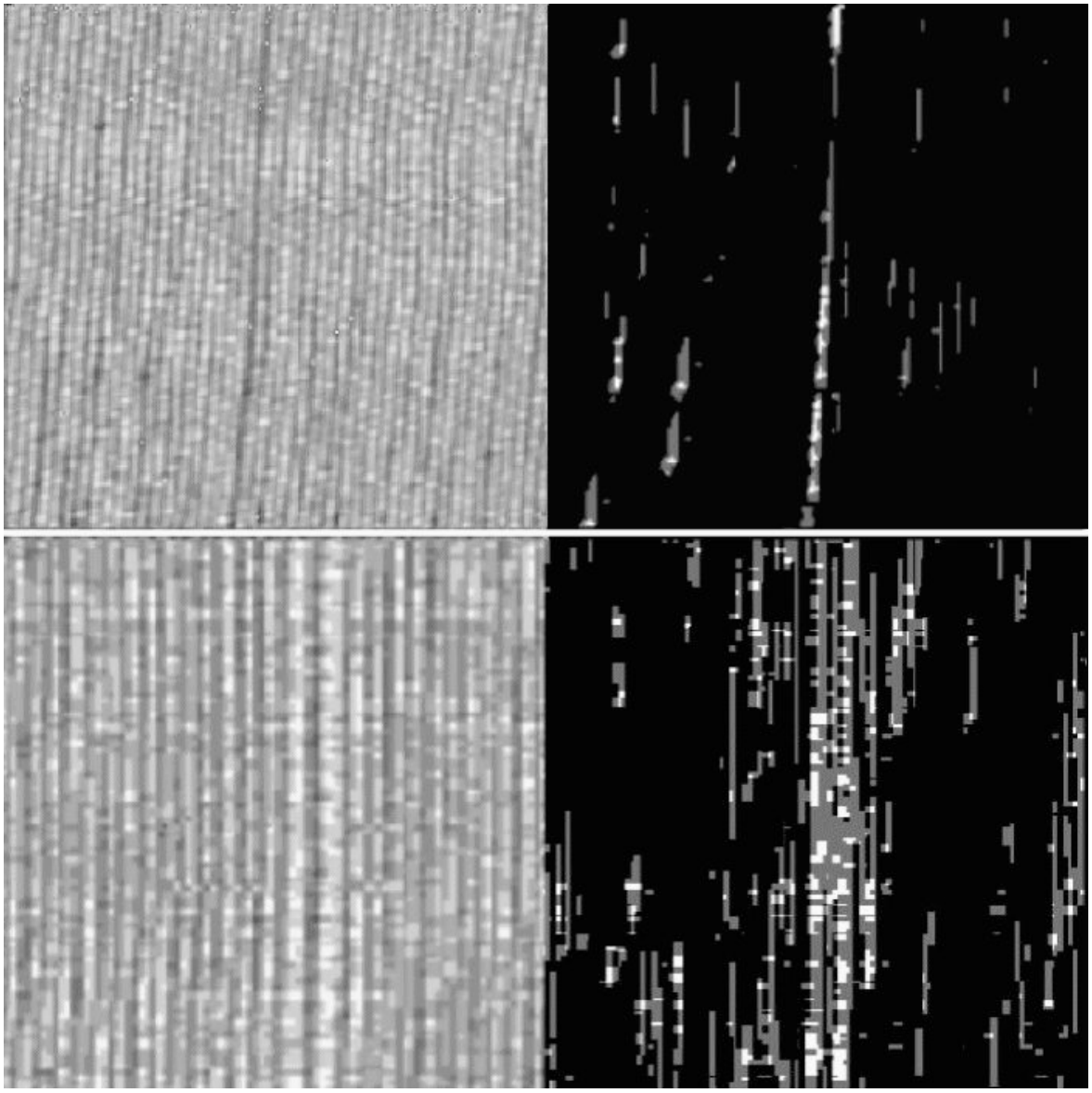

Figure 4: Doublepicks in fabrics are rather difficult to check (upper part) but the fault map is able to put in evidence this defect. In the lower part, a missing pick which is a quite common defect in fabrics. (Image sizes are 30 mm for the upper images and 20 mm for the lower images).

deviations from the recurrence of a fundamental unit, and usually appear as subtle lines, dark or bright, in the image frame. The more frequently encountered defects are broken or missing picks. Dust, extraneous staples or oil spots can also be observed. Monitoring of textile surfaces with statistical methods was recently proposed [7,8]. Starting from coherence lengths, fault detection can be done by the following procedure.

Sizes of the fundamental unit is determined by means of the coherence lengths, L_o^x, L_o^y. Then, windowing with L_o^x and L_o^y on each point of the image, we compare the local mean value with the global value M_o:

$$\Sigma_x(x,y) = \frac{1}{L_o^x} \sum_{\xi=0}^{L_o^x} \left[g(x+\xi, y) - M_o \right]^2 \tag{5}$$

$$\Sigma_y(x,y) = \frac{1}{L_o^y} \sum_{\chi=0}^{L_o^y} \left[g(x, y+\chi) - M_o \right]^2 \tag{6}$$

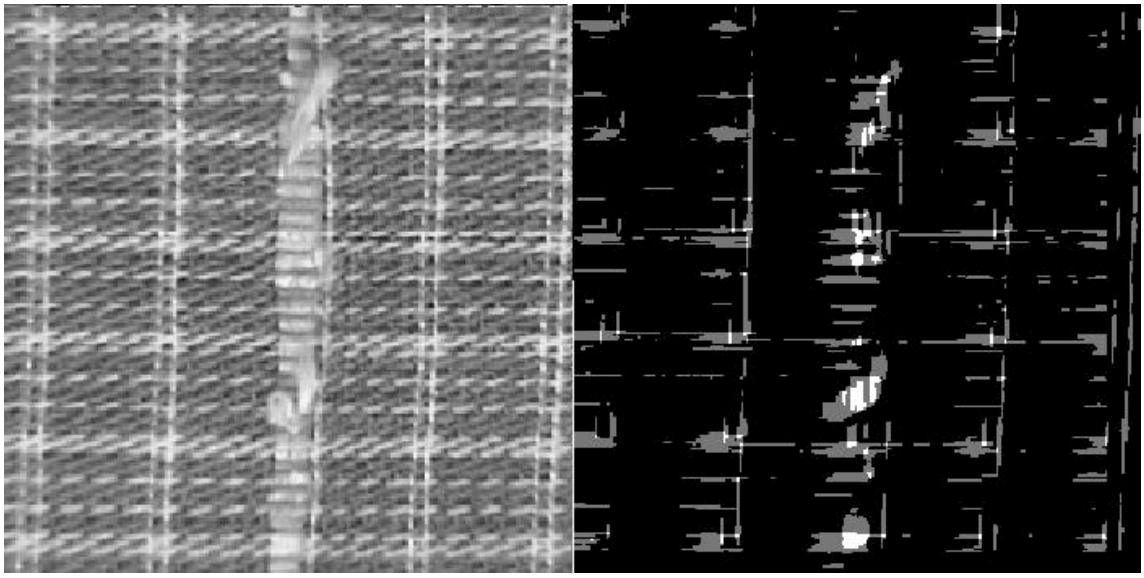

Figure 5: Defect in a complex fabrics with yarns of different colors. The fault map is able to find defects also in this case. Image size is 20 mm.

Functions Σ_x, Σ_y are suggested by the experimental observations on textile samples that defects are occupying one or more fundamental units, producing regions in the image where pixel tones have statistical moments very different from the moments of the whole image.

$\Sigma_x(x,y)$, $\Sigma_y(x,y)$ are functions of the image point $P(x,y)$ and can be used to obtain maps relevant to defect monitoring, associating grey tones to function values. For instance, bright pixels can mark the defective positions. To decide whether a pixel is in a fault or not, functions $\Sigma_x^{1/2}(x,y)$, $\Sigma_y^{1/2}(x,y)$ are compared with $M_2^{1/2}$, within a certain threshold. In the textile fault detection examples shown in next section, if both values $\Sigma_x^{1/2}(x,y)$, $\Sigma_y^{1/2}(x,y)$ differ from $M_2^{1/2}$ of more than 50%, pixel is marked as white. If only one is exciding the threshold, it is marked as grey. Black points are non defective points.

4 Discussion and conclusions

Only few parameters, all deducible from the image under consideration, are involved in the algorithm monitoring the presence of defects. Comparisons with a reference image or 'a priori' fixed parameters are not required. Moreover, the algorithm does not require high quality images that are hardly to obtain in applications where camera distances and illumination systems are strongly conditioned by the environment. In upper part of Figure 3, a textile surface with a mispick and the corresponding map are reproduced. The fault map was obtained with the procedure proposed in the previous section. Mispick is a rather common defect, produced when a yarn is lacking or broken on the loom, and it is a defect expanding on the surface fabric and involving several neighbour yarns. Mispicks are easy to find by eye inspection.

In upper right part of Fig.3, it is shown how our algorithm marks only defects and is not suffering of the local intensity variation, easily found on textile surfaces. In the map, we used only three grey levels for simplicity: black for pixels in the fabric area without defects, white for very defective points, and grey for intermediate defective signal. In the lower part of Figure 3, the same material with dust and little oil spots is shown. Mispicks, dust and spots are eye-inspected with back lighting and the same illumination system was used to record images.

In fabric production, defects that are rather difficult to identify are the doublepicks, appearing when two yarns are very close. Unlike mispick, this defect produces a very narrow line in the fabric, nevertheless, rather visible by eye inspection with back lighting illumination. A doublepick is shown in the upper part of Fig.4, with the corresponding defect map. In the lower part of the figure a mispick in the asem fabric.

Other fault detection examples are shown in the following Figures 5 and 6, which show the map of

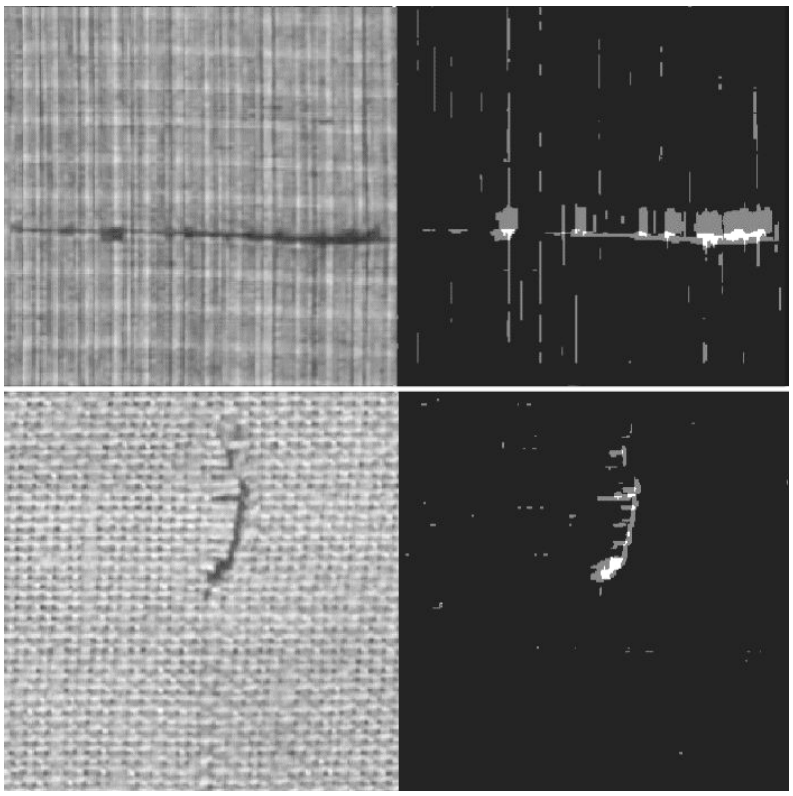

Figure 6: High contrast defects are easily detected by the fault map.

fault detection working on a sample with yarns of different colors (Fig.5) and a strong evidence of detection in the case of faults with high contrast (Fig.6) respectively.

Once the sizes of fundamental units in the textile surface are determined with coherence lengths, several statistical analysis can be performed, defining "faults" [12] in different manners, according to the statistical moment chosen for comparison between local and global values.

References:

[1] H. Sari-Sarraf, and J.S. Goddard, Vision systems for on-loom fabric inspection, IEEE Trans. Industry applications, 35, 1252-1259 (1999).

[2] J.G. Campbell and F. Murtagh, Automatic vision inspection of woven textiles using a two-stage defect detector, Opt. Eng. 37, 2536-2542 (1998).

[3] H.F. Yau, P.W. Chen, N.C. Wang, and Y.L. Lay, Optimization of the illumination beam size of an optical textile defect inspection system, Meas. Sci. Technol. 9, 960-966 (1998).

[4] S. Ribolzi, J. Merckle, and J.Gresser, Real time fault detection on textiles using opto-electronic processing, Textile Res. J. 63, 61-71 (1993).

[5] H.L. Kasdan, Industrial application of diffraction pattern sampling, Opt. Eng. 18, 496-503 (1979)

[6] R.M. Haralick, K. Shanmugam, K., and I. Dinstein, Textural features for image classification, IEEE Trans. Syst., Man, Cybern., SMC-3, 610-21 (1973).

[7] A. Abouelela, I. Abbas, I. El deeb, and S. Nassar, A statistical approach for textile fault detection, IEEE International Conference on Systems, Man, and Cybernetics, 8-11 Oct. 2000, 4, 2857-2862 (2000).

[8] A. Kumar, and G.K.H. Pang, Defect detection in textured materials using Gabor filters, Industry Applications, IEEE Transactions on Industry Applications, 38, 425-440 (2002).

[9] C.H. Chan and G. Pang, Fabric defect detection by Fourier analysis, IEEE Transactions on Industry Applications, 36, 1267-1276 (2002).

[10] J.W. Jasper, S.J. Garnier, and H. Potlapalli, Texture characterization and defect detection using adaptive wavelets, Opt. Eng., 35, 3140-3149 (1996).

[11] B. Montrucchio, A. Sparavigna, and A. Strigazzi, A new image processing method for enhancing the detection sensitivity of smooth transitions in liquid crystals, Liq. Cryst., 24, 841-852 (1998).

[12] Textile surfaces and fault maps are reproduced at http://staff.polito.it/amelia.sparavigna/faults.